

# Asymmetric Duffing oscillator: jump manifold and border set

Jan Kyzioł, Andrzej Okniński  
Politechnika Świętokrzyska, Al. 1000–lecia PP 7,  
25-314 Kielce, Poland

March 11, 2022

## Abstract

We study the jump phenomenon present in the forced asymmetric Duffing oscillator using the known steady-state asymptotic solution. The major result is the computation of the jump manifold, which encodes global information about all possible jumps.

## 1 Introduction

In this work we study steady-state dynamics of the forced asymmetric Duffing oscillator governed by the equation:

$$\ddot{y} + 2\zeta\dot{y} + \gamma y^3 = F_0 + F \cos(\Omega t), \quad (1)$$

where  $\zeta$ ,  $\gamma$ ,  $F_0$ ,  $F$  are parameters and  $\Omega$  is the angular frequency of the periodic force, which has a single equilibrium position and a corresponding one-well potential [1]. This dynamical system in particular and Duffing-type equations in general, which can be used to describe pendulums, vibration absorbers, beams, cables, micromechanical structures, and electrical circuits, have a long history [2]. The equation of motion (1) can describe several non-linear phenomena, such as various non-linear resonances, symmetry breaking, chaotic dynamics, period-doubling route to chaos, multistability and fractal dependence on initial conditions, and jumps [2–6].

The aim of our work is to research the jump phenomenon described and investigated for the system (1) in an interesting study by Kovacic and Brennan [1], using the implicit function machinery. An early approach to the jump phenomenon is due to Holmes and Rand [7] in the Catastrophe Theory setting where a discriminant of a cubic equation, arising in the amplitude-frequency response function, was analysed to detect multivaluedness of the amplitude. Recently, Kalmár-Nagy and Balachandran applied a differential condition to detect vertical tangencies, characteristic for the jump phenomenon [8].

In the next Section we describe the steady state solution (2) [1,6,9] which is an implicit function of  $A_0$  and  $\Omega$  (5) and compute an implicit function of  $A_1$  and  $\Omega$  (6a), (6b). Working in the framework developed in our earlier papers [10,11] we compute the jump manifold in Section 4 containing information about all possible jumps which is the main achievement of this work. We summarize our results in the last Section.

## 2 The steady-state solution

The steady-state solution of Eq. (1) of form:

$$y(t) = A_0 + A_1 \cos(\Omega t + \theta), \quad (2)$$

can be computed by any of asymptotic methods to yield non-linear algebraic equations expressing variables  $A_0, A_1, \theta$  and  $\Omega$  by parameters  $\zeta, \gamma, F_0, F$  [1,6,9]:

$$-A_1 \Omega^2 + 3\gamma A_0^2 A_1 + \frac{3}{4}\gamma A_1^3 - F \cos \theta = 0, \quad (3a)$$

$$-2\zeta A_1 \Omega - F \sin \theta = 0, \quad (3b)$$

$$\gamma A_0^3 + \frac{3}{2}\gamma A_0 A_1^2 - F_0 = 0. \quad (3c)$$

Eliminating  $\theta$  from Eqs. (3a), (3b) we get two implicit equations for  $A_0, A_1$  and  $\Omega$ :

$$A_1^2 \left( -\Omega^2 + 3\gamma A_0^2 + \frac{3}{4}\gamma A_1^2 \right)^2 + 4\Omega^2 \zeta^2 A_1^2 = F^2, \quad (4a)$$

$$\gamma A_0^3 + \frac{3}{2}\gamma A_0 A_1^2 - F_0 = 0. \quad (4b)$$

Computing  $A_1^2$  from Eq. (4b) and substituting into (4a) we obtain an implicit equation for  $A_0, \Omega$ :

$$f(\Omega, A_0; \gamma, \zeta, F, F_0) = \sum_{k=0}^9 c_k A_0^k = 0, \quad (5)$$

where coefficients  $c_k$  are given in Table 1.

Table 1: Coefficients of polynomial (5)

$c_9 = 25\gamma^3$	$c_4 = 16\Omega^2\gamma F_0$
$c_8 = 0$	$c_3 = -9\gamma F_0^2 + 6\gamma F^2$
$c_7 = -20\Omega^2\gamma^2$	$c_2 = -4F_0\Omega^4 - 16\zeta^2\Omega^2 F_0$
$c_6 = -15\gamma^2 F_0$	$c_1 = 4\Omega^2 F_0^2$
$c_5 = -15\gamma^2 F_0$	$c_0 = -F_0^3$

We can also obtain implicit equation for  $A_1$ ,  $\Omega$ . We solve the cubic equation Eq. (4b) for  $A_0$  computing one real root (two other roots are complex):

$$A_0 = -\frac{A_1^2}{2Y} + Y, \quad Y \equiv \sqrt[3]{\sqrt{\frac{1}{8}A_1^6 + \frac{1}{4\gamma^2}F_0^2} + \frac{1}{2\gamma}F_0}. \quad (6a)$$

Then we substitute  $A_0$  from Eq. (6a) into Eq. (4a), obtainig finally a complicated but useful implicit equation for  $A_1$ ,  $\Omega$ :

$$g(\Omega, A_1; \gamma, \zeta, F, F_0) = A_1^2 (3\gamma A_0^2 + \frac{3}{4}\gamma A_1^2 - \Omega^2)^2 + 4\Omega^2 \zeta^2 A_1^2 - F^2 = 0, \quad (6b)$$

where  $A_0$  and  $Y$  are defined in (6a).

### 3 Singular points

Conditions for singular points are [10, 11]:

$$f(\Omega, A_0; \gamma, \zeta, F, F_0) = 0, \quad (7a)$$

$$\frac{\partial f(\Omega, A_0; \gamma, \zeta, F, F_0)}{\partial \Omega} = 0, \quad (7b)$$

$$\frac{\partial f(\Omega, A_0; \gamma, \zeta, F, F_0)}{\partial A_0} = 0. \quad (7c)$$

Since the derivative  $\frac{\partial}{\partial \Omega} f(\Omega, A_0, \gamma, \zeta, F, F_0)$  factorizes:

$$\frac{\partial f(\Omega, A_0; \gamma, \zeta, F, F_0)}{\partial \Omega} = 8A_0\Omega (F_0 - \gamma A_0^3) (F_0 + A_0 (5\gamma A_0^2 - 4\delta^2 - 2\Omega^2)) \quad (8)$$

we get from Eq. (7b):

$$F_0 = 2\Omega^2 A_0 + 4\zeta^2 A_0 - 5\gamma A_0^3, \quad (9)$$

other possibilities leading to trivial solutions or cases without a solution.

Substituting (9) into Eqs. (7a), (7c) we obtain:

$$256\zeta^4 X^4 + 1280\zeta^6 X^3 + (-96c\zeta^2 + 2304\zeta^8) X^2 + (-336c\zeta^4 + 1792\zeta^{10}) X + 512\zeta^{12} - 240\zeta^6 c + 45c^2 = 0, \quad (10a)$$

$$\frac{1}{45F^2\gamma^2} A_0^2 = 16\zeta^2 X^3 + 64\zeta^4 X^2 + (9\gamma F^2 + 80\zeta^6) X + 15\gamma F^2 \zeta^2 + 32\zeta^8. \quad (10b)$$

where  $X = \Omega^2$ ,  $c = \gamma F^2$ .

We have checked, plotting the implicit function of  $X$ ,  $\zeta$ ,  $c$  defined by Eq. (10a), that Eq. (10a) has no solutions  $X = \Omega^2 > 0$ . We thus conclude that the system of equations (4) has no singular points.

## 4 The jump phenomenon

### 4.1 Jump conditions and jump manifold

Jump conditions in implicit function setting read [10, 11]:

$$f(\Omega, A_0; \gamma, \zeta, F, F_0) = 0, \quad (11a)$$

$$\frac{\partial f(\Omega, A_0; \gamma, \zeta, F, F_0)}{\partial A_0} = 0. \quad (11b)$$

where equation (11b) is the condition for a vertical tangency (note that equations (11) are Eqs. (7a), (7c)).

Solving equations (11) we obtain:

$$J(A_0; \gamma, \zeta, F, F_0) = \sum_{k=0}^{21} a_k A_0^k = 0, \quad (12a)$$

$$\Omega^2 = \frac{(-50\gamma^4)A_0^{12} + 95\gamma^3 F_0 A_0^9 + (6F^2\gamma^2 - 39\gamma^2 F_0^2)A_0^6 + (3F^2\gamma F_0 - 7\gamma F_0^3)A_0^3 + F_0^4}{2A_0(F_0 - 10\gamma A_0^3)(F_0 - \gamma A_0^3)^2}, \quad (12b)$$

the non-zero coefficients  $a_k$  of the polynomial  $J(A_0)$  given in Table 2.

Table 2: Non-zero coefficients of polynomial (12a)

$a_{21} = 4000\gamma^7\zeta^2$	$a_9 = 3248\gamma^3\zeta^2 F_0^4 - 72F^2\gamma^3\zeta^2 F_0^2$
$a_{18} = -16000\gamma^6\zeta^2 F_0$	$a_8 = 36F^4\gamma^3 F_0 - 978F^2\gamma^3 F_0^3$
$a_{17} = 600F^2\gamma^6$	$a_6 = 528\gamma^2\zeta^2 F_0^5 - 240F^2\gamma^2\zeta^2 F_0^3$
$a_{15} = 23880\gamma^5\zeta^2 F_0^2 - 480F^2\gamma^5\zeta^2$	$a_5 = 9F^4\gamma^2 F_0^2 + 138F^2\gamma^2 F_0^4$
$a_{14} = -1920F^2\gamma^5 F_0$	$a_3 = 24F^2\gamma\zeta^2 F_0^4 - 152\gamma\zeta^2 F_0^6$
$a_{12} = 768F^2\gamma^4\zeta^2 F_0 - 15512\gamma^4\zeta^2 F_0^3$	$a_2 = -6F^2\gamma F_0^5$
$a_{11} = 36F^4\gamma^4 + 2166F^2\gamma^4 F_0^2$	$a_0 = 8\zeta^2 F_0^7$

The polynomial  $J(A_0)$ , complicated as it is, encodes global information about all possible jumps. We shall thus refer to equation (12a), which defines an implicit function of variables  $A_0, \gamma, \zeta, F, F_0$ , as jump manifold equation. Thus, the jump manifold  $\mathcal{J}(A_0, \gamma, \zeta, F, F_0)$ :

$$\mathcal{J}(A_0, \gamma, \zeta, F, F_0) = \{(A_0, \gamma, \zeta, F, F_0) : J(A_0; \gamma, \zeta, F, F_0) = 0\}, \quad (13)$$

belongs to  $5D$  space. It is purposeful to introduce projection of the jump manifold onto the parameter space:

$$\mathcal{J}_\perp(\gamma, \zeta, F, F_0) = \{(\gamma, \zeta, F, F_0) : \text{there is such } A_0 \text{ that } J(A_0; \gamma, \zeta, F, F_0) = 0\}. \quad (14)$$

In other words, for any set of parameters  $\gamma, \zeta, F, F_0$  belonging to  $\mathcal{J}_\perp$  there is a jump in dynamical system (1) and all jumps occur for parameters belonging to  $\mathcal{J}_\perp$ .

We shall consider  $2D$  and  $3D$  projections, plotting  $\mathcal{J}(A_0; \gamma_*, \zeta_*, F_*, F_0)$  and  $\mathcal{J}(A_0; \gamma_*, \zeta_*, F, F_0)$ , respectively, where parameters  $\gamma_*, \zeta_*, F_*$  or  $\gamma_*, \zeta_*$  are fixed.

#### 4.1.1 2D projection, $J(A_0; \gamma_*, \zeta_*, F_*, F_0) = 0$

Global picture of the jump manifold  $\mathcal{J}(A_0; \gamma_*, \zeta_*, F_*, F_0)$  where  $\gamma_* = 0.0783$ ,  $\zeta_* = 0.025$ ,  $F_* = 0.1$  and  $A_0, F_0$  are variable is shown in Fig. 1.

Firstly, all points lying on the blue curve correspond to jumps. Moreover, there are four critical points, dividing Fig. 1 into parts and referred to as *border points*:  $F_0^{(1)} = 0$ ,  $F_0^{(2)} = 0.0920$ ,  $F_0^{(3)} = 0.7385$ ,  $F_0^{(4)} = 6.5321$ , defined and computed in the Subsection 4.2. It turns out that  $F_0 \in (F_0^{(1)}, F_0^{(2)})$  there are two vertical tangencies, for  $F_0 \in (F_0^{(2)}, F_0^{(3)})$  there are four, for  $F_0 \in (F_0^{(3)}, F_0^{(4)})$  there are two and there are no vertical tangencies for  $F_0 > F_0^{(4)}$ .

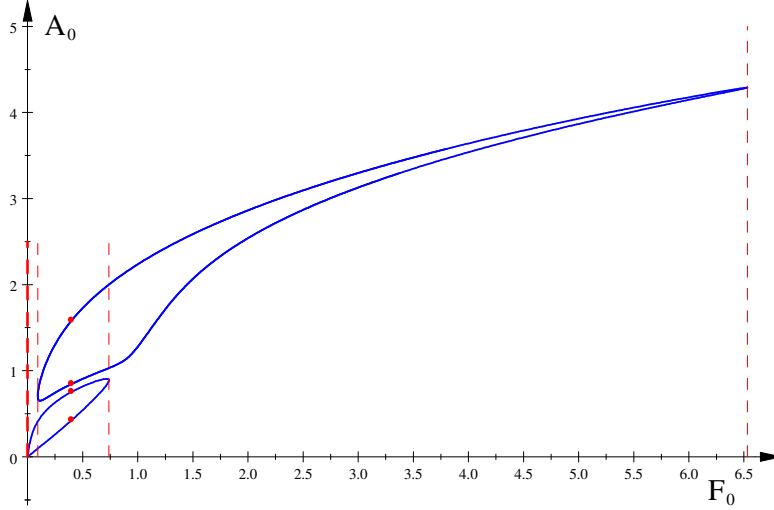


Figure 1: Jump manifold  $\mathcal{J}(A_0; \gamma_*, \zeta_*, F_*, F_0)$ ,  $\gamma_* = 0.0783$ ,  $\zeta_* = 0.025$ ,  $F_* = 0.1$  (blue) and four border points on intersections of  $\mathcal{J}$  and vertical red lines.

For example, in Fig. 2 the case  $F_0 = 0.4$  is shown. More exactly, the implicit function  $A_1(\Omega)$ , computed with help of Eq. (6b) is plotted for  $\gamma = 0.0783$ ,  $\zeta = 0.025$ ,  $F = 0.1$  and  $F_0 = 0.4$ . Red dots, denoting vertical tangencies, correspond to red dots in Fig. 1. These points can be easily computed from Eqs. (11), (4).

Indeed, solving equations (11) for  $\gamma = 0.0783$ ,  $\zeta = 0.025$ ,  $F = 0.1$ ,  $F_0 = 0.4$  we get four real solutions  $\Omega$ ,  $A_0$  shown in the first two column in Table 3. Then for the above values of  $\Omega$  we solve equations (4) obtaining four values of  $A_1$  listed in the third column of the Table 3.

Table 3: Solutions of Eqs. (11) and (4)

$\Omega$	$A_0$	$A_1$
0.576 122 891	0.846 633 527	1. 882 759 746
0.643 209 846	0.755 260 872	2. 032 001 367
0.690 545 624	1. 583 776 750	0.691 474 188
0.711 882 658	0.425 889 574	2. 806 379 023

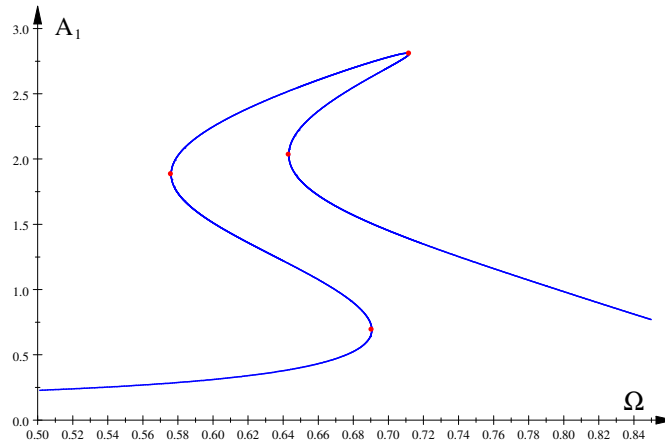


Figure 2: Amplitude-frequency response curve  $A_1(\Omega)$ ,  $\gamma = 0.0783$ ,  $\zeta = 0.025$ ,  $F = 0.1$ ,  $F_0 = 0.4$ .

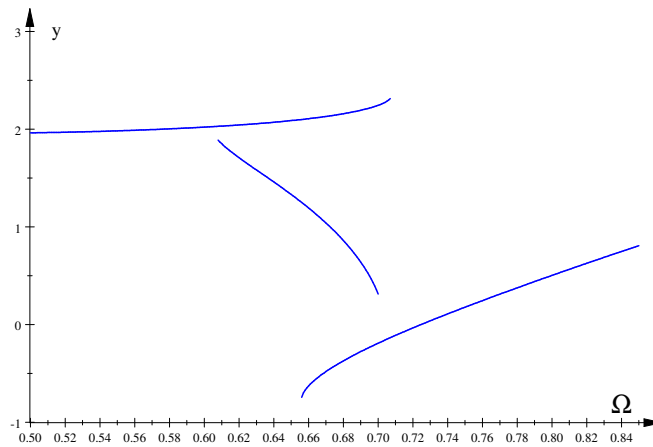


Figure 3: Bifurcation diagram,  $\gamma = 0.0783$ ,  $\zeta = 0.025$ ,  $F = 0.1$ ,  $F_0 = 0.4$ .

In Fig. 3 the bifurcation diagram is shown for the set of parameters listed

in Fig. 2. Note good agreement of end points of bifurcation branches in Fig. 3 with  $\Omega$  coordinates of red dots in Fig. 2.

#### 4.1.2 3D projection, $J(A_0; \gamma_*, \zeta_*, F, F_0) = 0$

We now fix two parameters only, for example  $\gamma_* = 0.0783$ ,  $\delta_* = 0.025$ , and plot the jump manifold  $\mathcal{J}(A_0; \gamma_*, \zeta_*, F, F_0)$  as a 3D surface, see Fig. 4.

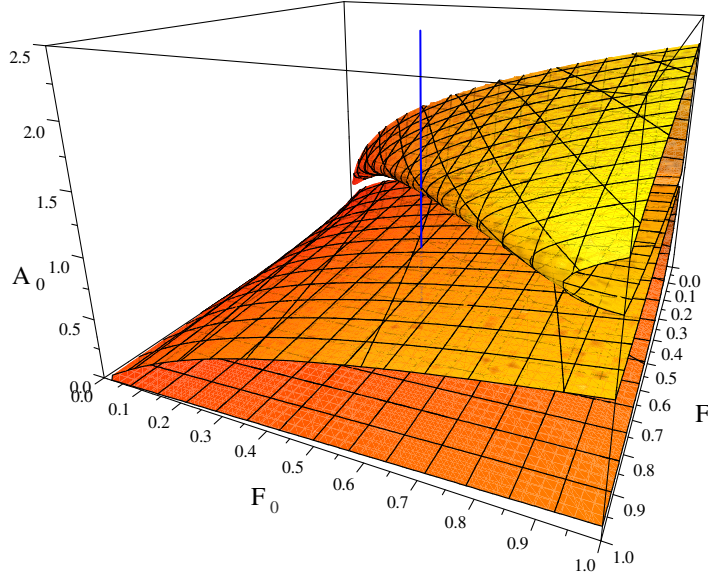


Figure 4: Jump manifold  $\mathcal{J}(A_0; \gamma_*, \zeta_*, F, F_0)$ ,  $\gamma_* = 0.0783$ ,  $\zeta_* = 0.025$ .

Next we compute one border point. For example, we choose  $F_0 = 0.5$  ( $\gamma_* = 0.0783$ ,  $\delta_* = 0.025$ ) and compute the corresponding border point as  $F = 0.544860$ ,  $A_0 = 1.238340$  as explained in the next Subsection.

The blue vertical line, given by the just computed data  $(0.544860, 0.5, A_0)$  with  $A_0$  variable, touches the upper lobe of the jump manifold exactly at the border point  $(0.544860, 0.5, 1.238340)$ .

## 4.2 Border sets

We shall now determine condition for the border set: the set of points in the parameter space  $(\gamma, \zeta, F, F_0)$ , such that number of vertical tangencies changes at these points. Condition for the border set is that the polynomial  $J(A_0)$  given in Eq. (12a) and Table 2 has multiple roots. Qualitative behaviour of the polynomial equation  $J(A_0)$  can be seen in Figs. 1, 2 where 2D and 3D projections of the implicit function  $J(A_0; \gamma, \zeta, F, F_0) = 0$  are shown. To find parameters' values for which the polynomial  $J(A_0; \gamma, \zeta, F, F_0)$  has multiple roots we demand that resultant of  $J(A_0)$  and its derivative  $J'(A_0) = \frac{d}{dA_0}J(A_0) =$

$\sum_{k=0}^{20} b_k A_0^k$  is zero [12, 13]:

$$R(J, J'; \gamma, \zeta, F, F_0) = 0. \quad (15)$$

Resultant of the polynomial (12a), Table 2 is a determinant of the  $(m+n) \times (m+n)$  Sylvester matrix,  $n = 21$ ,  $m = 20$ :

$$R(J, J'; \gamma, \zeta, F, F_0) = \det \begin{pmatrix} a_n & a_{n-1} & a_{n-2} & \dots & 0 & 0 & 0 \\ 0 & a_n & a_{n-1} & \dots & 0 & 0 & 0 \\ \vdots & \vdots & \vdots & & \vdots & \vdots & \vdots \\ 0 & 0 & 0 & \dots & a_1 & a_0 & 0 \\ 0 & 0 & 0 & \dots & a_2 & a_1 & a_0 \\ b_m & b_{m-1} & b_{m-2} & \dots & 0 & 0 & 0 \\ 0 & b_m & b_{m-1} & \dots & 0 & 0 & 0 \\ \vdots & \vdots & \vdots & & \vdots & \vdots & \vdots \\ 0 & 0 & 0 & \dots & b_1 & b_0 & 0 \\ 0 & 0 & 0 & \dots & b_2 & b_1 & b_0 \end{pmatrix} \quad (16)$$

and is an enormously complicated polynomial in variables  $\gamma$ ,  $\zeta$ ,  $F_0$ ,  $F$ . However, if we fix three parameters, say  $\gamma$ ,  $\zeta$ ,  $F$ , then the equation  $R(J, J') = 0$  can be solved numerically and thus critical values of  $F_0$  can be computed.

For example, we have solved equation (15),  $R(J, J'; \gamma_*, \zeta_*, F_*, F_0) = 0$ , for

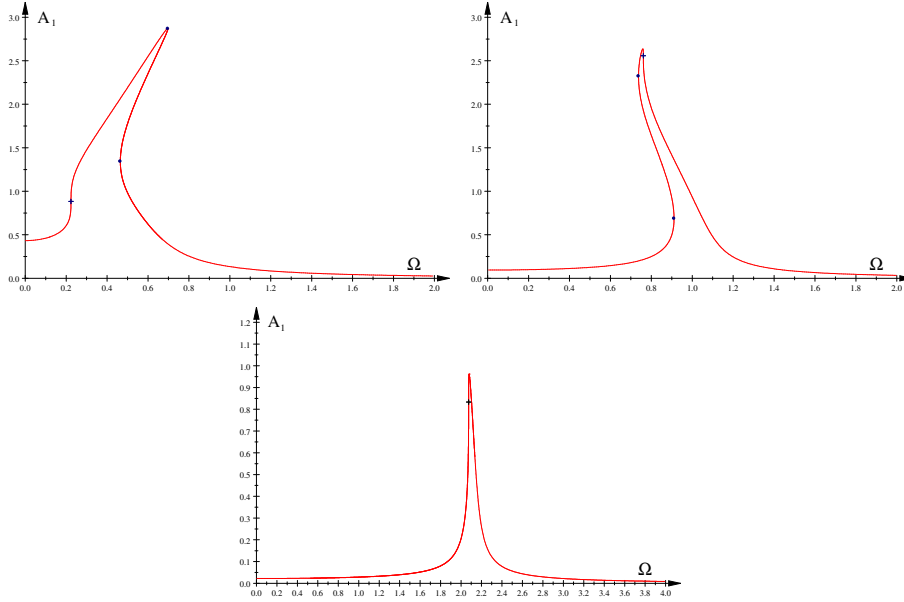


Figure 5: Amplitude-frequency response curves:  $\gamma = 0.0783$ ,  $\zeta = 0.025$ ,  $F = 0.1$ ,  $F_0^{(2)} = 0.092$  (left top),  $F_0^{(3)} = 0.7385$  (right top),  $F_0^{(4)} = 6.532$  (bottom).



$\gamma_* = 0.0783$ ,  $\zeta_* = 0.025$ ,  $F_* = 0.1$  obtaining the following real positive solutions:  $F_0^{(1)} = 0$ ,  $F_0^{(2)} = 0.092075$ ,  $F_0^{(3)} = 0.738510$ ,  $F_0^{(4)} = 6.532092$ . In Figs. 5 border amplitudes for  $\gamma = 0.0783$ ,  $\zeta = 0.025$ ,  $F = 0.1$  and  $F_0^{(2)}$ ,  $F_0^{(3)}$ ,  $F_0^{(4)}$  are marked with blue crosses, respectively. Blue dots denote points of jumps.

We have also solved equation (15),  $R(J, J'; \gamma_*, \zeta_*, F, F_{0*}) = 0$ , for  $\gamma_* = 0.0783$ ,  $\zeta_* = 0.025$ ,  $F_{0*} = 0.5$  obtaining real positive solutions:  $F^{(1)} = 0$ ,  $F^{(2)} = 0.0269989$ ,  $F^{(3)} = 0.0779256$ ,  $F^{(4)} = 0.5448595$ . Next, for  $\gamma = 0.0783$ ,  $\zeta = 0.025$ ,  $F_0 = 0.5$ , and  $F = 0.5448595$  we have computed from Eqs. (11) the border value  $A_0 = 1.238340$ , see the blue vertical line in Fig. 4.

### 4.3 Number of solutions of Eq. (5) for a given value of $\Omega$

There are also other qualitative changes of the amplitudes  $A_1(\Omega)$  controlled by the parameters. For example, number of solutions of Eq. (5) for a given value of  $\Omega$  may change. This happens when two vector tangencies appear at the same value of  $\Omega$ . For example, let  $\gamma = 0.0783$ ,  $\zeta = 0.025$ ,  $F = 0.1$ . To find a value of  $F_0$  for which this happens we have to find a double root of  $\Omega$  of equations (11). Therefore, solving Eqs. (11) numerically for several values of  $F_0$  we easily find that for  $F_0 = 0.301007$  there is indeed a double root:  $\Omega = 0.597114$ ,  $A_0 = 0.679284$  and  $\Omega = 0.597114$ ,  $A_0 = 1.411787$ . There is another such case, for  $F_0 = 0.429166$  there is a double root:  $\Omega = 0.714419$ ,  $A_0 = 0.459118$  and  $\Omega = 0.714419$ ,  $A_0 = 1.628271$ .

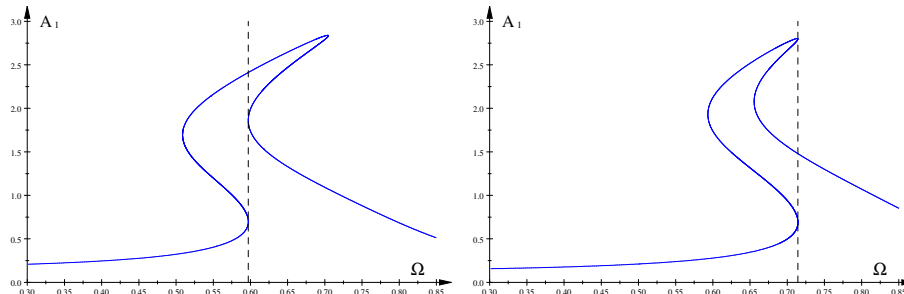


Figure 6: Amplitude-frequency response curves  $A_1(\Omega)$ :  $\gamma = 0.0783$ ,  $\zeta = 0.025$ ,  $F = 0.1$ ,  $F_0 = 0.301$  (left),  $F_0 = 0.429$  (right).

Therefore, for  $F_0 \in (0.301, 0.429)$  equation (5) has five solutions.

## 5 Summary

Working in the implicit function framework [10, 11], we have computed in Subsection 4.1, using the (approximate) steady-state solution obtained in [1, 6, 9], the jump manifold 13, comprising information about all jumps in the dynamical system 1. Our formalism, described in Section 4 – built on an idea to use

a differential condition to detect vertical tangencies, due to Kalmár-Nagy and Balachandran [8] – can be applied to arbitrary steady-state solution.

Our work on the asymmetric Duffing oscillator is a supplementation and amplification of results obtained by Kovacic and Brennan [1]. More precisely, the sequence of figures 8.4 (a) –(e), computed in [1] for  $\gamma = 0.0783$ ,  $\zeta = 0.025$ ,  $F = 0.1$  and  $F_0 = 0.01, 0.2, 0.4, 0.5, 0.95$ , respectively, can be appended with Figs. 5 and 6, computed for  $F_0 = 0.092, 0.7385, 6.532$  and  $F_0 = 0.301, 0.429$ . Therefore, the whole sequence of metamorphoses of the curve  $A_1(\Omega)$  consists of plots computed for  $F_0 = \mathbf{0.01}, 0.092, \mathbf{0.2}, 0.301, \mathbf{0.4}, 0.429, \mathbf{0.5}, 0.7385, \mathbf{0.95}, 6.532$  where numbers highlighted in bold correspond to Figs. 8.4 (a) – (e) plotted in [1].

## References

- [1] Kovacic, I., Brennan, M.J. Forced harmonic vibration of an asymmetric Duffing oscillator. In *The Duffing Equation: Nonlinear Oscillators and Their Behavior* (Kovacic, I., Brennan, M.J., eds.); John Wiley & Sons, Hoboken, New Jersey 2011; pp. 277 – 322.
- [2] Kovacic, I., Brennan, M.J. (eds.) *The Duffing Equation: Nonlinear Oscillators and Their Behavior*; John Wiley & Sons, Hoboken, New Jersey 2011.
- [3] C. Hayashi, *Nonlinear Oscillations in Physical Systems*, McGraw-Hill, New York, 1964.
- [4] Y. Ueda, Explosions of strange attractors exhibited by Duffing equation. *Ann. N.Y. Acad. Sci.* **357** (1980) 422 –4 33.
- [5] Y. Ueda, Randomly transitional phenomena in the systems governed by Duffing’s equation. *J. Stat. Phys.* **20** (1979) 181 – 196.
- [6] Szemplińska-Stupnicka, W., Bajkowski, J. The 1/2 subharmonic resonance and its transition to chaotic motion in a non-linear oscillator. *Int. J. Non-Linear mechanics* **21**(5) (1986) 401 – 419.
- [7] Holmes, P.J.; Rand, D.A. The bifurcations of Duffing’s equation: An application of Catastrophe Theory. *J. Sound Vib.* **44** (1976) 237 – 253.
- [8] Kalmár-Nagy, T.; Balachandran, B. Forced harmonic vibration of a Duffing oscillator with linear viscous damping. In *The Duffing Equation: Nonlinear Oscillators and Their Behavior*; (Kovacic, I., Brennan, M.J., eds.); John Wiley & Sons, Hoboken, New Jersey 2011; pp. 139 – 174.
- [9] D.W. Jordan, P. Smith, *Nonlinear Ordinary Differential Equations*, Oxford University Press, New York, 1999.
- [10] Kyzioł, J., Okniński, A. Duffing-type equations: singular points of amplitude profiles and bifurcations, *Acta Phys. Polon. B* **52** (2021) 1239-1262.

- [11] Kyzioł, J., Okniński, A. Localizing Bifurcations in Non-Linear Dynamical Systems via Analytical and Numerical Methods, *Processes* **10** (2022) 127, 17 pages.
- [12] Gelfand, I.M., Kapranov, M.M., Zelevinsky, A.V. *Discriminants, Resultants, and Multidimensional Determinants*, Springer Science & Business Media, 2008.
- [13] Janson, S. Resultant and discriminant of polynomials, Lecture notes, <http://www2.math.uu.se/~protect\char126\relaxsvante/papers/sjN5.pdf>, 2010.